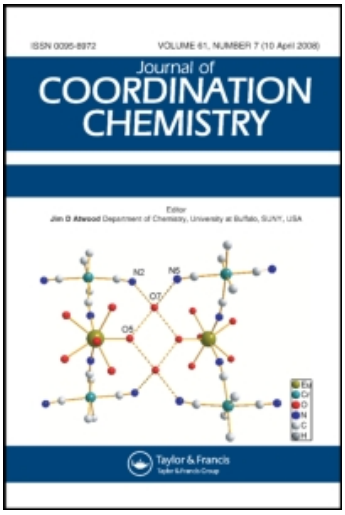

Journal of Coordination Chemistry
Publication details, including instructions for authors and subscription information:
http://www.informaworld.com/smpp/title~content=t713455674

Aqueous solution and solid state study of the chlorotris(1,3,5-triaza-7-phosphabicyclo[3.3.1.1^{3,7}]decane)platinum(II) ion and the crystal structure of {[Pt(NCS)(PTA)$_3$]NCS}$_3$·5H$_2$O

Zolisa A. Sam[a]; Andreas Roodt[a]; Stefanus Otto[a]
[a] Department of Chemistry, University of the Free State, Bloemfontein, 9300, South Africa

To cite this Article Sam, Zolisa A. , Roodt, Andreas and Otto, Stefanus(2006) 'Aqueous solution and solid state study of the chlorotris(1,3,5-triaza-7-phosphabicyclo[3.3.1.1^{3,7}]decane)platinum(II) ion and the crystal structure of {[Pt(NCS)(PTA)$_3$]NCS}$_3$·5H$_2$O', Journal of Coordination Chemistry, 59: 9, 1025 — 1036
To link to this Article: DOI: 10.1080/00958970500410416
URL: http://dx.doi.org/10.1080/00958970500410416

Journal of Coordination Chemistry
Vol. 59, No. 9, 15 June 2006, 1025–1036

Aqueous solution and solid state study of the chlorotris(1,3,5-triaza-7-phosphabicyclo[3.3.1.1^{3,7}]decane)-platinum(II) ion and the crystal structure of $\{[Pt(NCS)(PTA)_3]NCS\}_3 \cdot 5H_2O$

ZOLISA A. SAM†, ANDREAS ROODT*† and STEFANUS OTTO†‡

†Department of Chemistry, University of the Free State, P.O. Box 339, Bloemfontein, 9300, South Africa

(*Received in final form 18 August 2005*)

Reaction of $[PtCl(PTA)_3]^+$ (PTA = 1,3,5-triaza-7-phosphabicyclo[3.3.1.1^{3,7}]decane) with halides and pseudohalides gives $[PtX(PTA)_3]^+$ ($X = Br^-$, N_3^- and NCS^-) in an equilibrium process. At 25°C, equilibrium constants are 3.3(7), 11(2) and 20(2) for Br^-, N_3^- and NCS^-, respectively. Protonation of $[PtCl(PTA)_3]^+$ results in the formation of *cis*-$[PtCl_2(PTA)_2]$. Two pK_a values $pK_{a1} = 2.1(1)$ and $pK_{a2} = 3.3(8)$ were obtained, corresponding to the protonation of $[PtCl(PTA)_3]Cl$ and *cis*-$[PtCl_2(PTA)_2]$, respectively. From an aqueous reaction mixture of $[PtCl(PTA)_3]Cl$ and NCS^-, crystals of $\{[Pt(NCS)(PTA)_3]NCS\}_3 \cdot 5H_2O$ were isolated. The compound crystallizes in the triclinic space group $P\bar{1}$ and its crystal structure has been determined. Three platinum cations, three thiocyanate counterions and five solvent water molecules are present in the asymmetric unit.

Keywords: Platinum(II); 1,3,5-Triaza-7-phosphabicyclo[3.3.1.1^{3,7}]decane; Halides; Pseudohalides; Equilibrium studies; Crystal structure

1. Introduction

Complexes formed from transition metals with functionalized water-soluble phosphines are important due to their potential catalytic activity. Catalyst recovery and recycle are crucial considerations in catalytic reactions of industrial processes that are catalysed homogeneously by expensive transition metal complexes. The development of transition metal reagents for use in aqueous solvent systems offers advantages for a wide variety of chemical processes ranging from large-scale industrial processes to fine organic synthesis. The use of water-soluble reagents for chemical manufacture can simplify catalyst–product separation and is also interesting because of the economy

*Corresponding author. Email: roodta.sci@mail.uovs.ac.za
‡Present address: Sasol Technology R&D, P.O. Box 1, Sasolburg, 1947, South Africa.

Journal of Coordination Chemistry
ISSN 0095-8972 print: ISSN 1029-0389 online © 2006 Taylor & Francis
DOI: 10.1080/00958970500410416

and the safety of using water as a solvent. Water-soluble catalysts act as a joint interface between homogeneous and heterogeneous catalysis, allowing simple separation of the product from the catalyst while retaining high activity and selectivity. Catalytic activity has been demonstrated for complexes containing the PTA ligand through a rhodium complex used in catalytic hydrogenation [1]. Studies have also been carried out [2] using other water-soluble phosphine ligands such as TPPMS (TPPMS = sodium salt of (*m*-sulfonatophenyl)diphenylphosphine) and TPPTS (TPPTS = trisodium salt of tris(*m*-sulfonatophenyl)phosphine) in homogeneous catalytic systems.

There has been interest in rendering organometallic complexes water-soluble [3]. This is generally achieved *via* coordination of hydrophilic ligands, which usually are functionalized tertiary phosphines. Most water-soluble phosphines have ligands with hydrophilic functional groups and are mainly used in the field of catalysis and for possible medical applications [4]. An important discovery in the area of water-soluble phosphine ligands is that of 1,3,5-triaza-7-phosphabicyclo[3.3.1.1^{3,7}]decane (PTA) which was first prepared in 1974 by Daigle and co-workers [5]. Further investigations were later conducted by the groups of Darensbourg [6] and Joó [7]. The solubility of this compound in water and its relative stability towards oxidation make it an unusual aliphatic phosphine [8], and the small cone angle of 118° suggests that it should be a good substitute for trimethylphosphine [9]. The PTA ligand is most valuable as it enables the synthesis of water-soluble complexes without the additional complication of introducing a charged species to the complex. In addition, PTA can be either protonated by Bronsted acids (HX) or methylated at one of the nitrogen atom sites to form [PTAH]X or [PTA(CH_3)]I [10]. Protonation or alkylation gives increased additional solubility in water.

2. Experimental

Infrared spectra were obtained using KBr disks between 4000–250 cm^{-1} with a Hitachi 270–50 spectrophotometer, while ^{1}H and ^{31}P NMR spectra were recorded on a Bruker 300 MHz spectrometer operating at 300 and 121.497 MHz, respectively. NMR spectra were recorded in D_2O and ^{1}H spectra were calibrated relative to the residual H_2O peak (4.63 ppm) while the ^{31}P spectra were referenced to 85% H_3PO_4 as internal standard in a capillary at 0 ppm. Electronic spectra were recorded using Hitachi 150-20 or Cary 50 Conc. spectrophotometers equipped with constant temperature water baths, ±0.1°C.

2.1. *Chemicals and synthesis*

All general chemicals were of analytical grade and used without further purification. Distilled water was used in all experiments and all measurements were carried out in air. The ligand 1,3,5-triaza-7-phosphabicyclo[3.3.1.1^{3,7}]decane (PTA) was synthesized according to a published procedure [11]. [PtCl(PTA)$_3$]Cl was prepared according to a known procedure [12], by addition of 3 equivalents of PTA to an aqueous mixture of *cis*- and *trans*-[Pt(Cl)$_2$(SMe$_2$)$_2$].

2.1.1. {[Pt(NCS)(PTA)$_3$]NCS}$_3$·5H$_2$O. An aqueous solution of [PtCl(PTA)$_3$]Cl (20 mg, 0.027 mmol) was treated with 1.5 equivalents of NaNCS (3.3 mg, 0.041 mmol). The solution was evaporated in a fume hood and the yellow residue

recrystallized from water to give crystals suitable for X-ray analysis (12 mg, 57%). IR: ν(SCN) 2080 cm^{-1}. ^1H NMR (300 MHz, D_2O): δ 4.46 (s, 6H), 4.32 (s, 6H). $^{31}P\{^1H\}$ NMR (121.497 MHz, D_2O): δ −58.05 (s, broad peak). Electronic spectrum (H_2O): $\lambda_{max} = 298$ nm, $\varepsilon = 6520\ M^{-1}\ cm^{-1}$.

2.1.2. [Pt(Br)(PTA)$_3$]Br. Upon addition of excess of LiBr (285 mg, 3.3 mmol) to an aqueous solution (2 cm^3) of [PtCl(PTA)$_3$]Cl (80 mg, 0.1 mmol), the colourless solution immediately turned dark yellow. Concentration of the solution to 1 cm^3 and addition of acetone yielded a white solid (62 mg, 69%). ^1H NMR (300 MHz, D_2O): δ 4.49 (d, 6H), 4.44 (s, 6H). $^{31}P\{^1H\}$ NMR (121.497 MHz, D_2O): δ −57.87 (td, due to the phosphorus atoms of the PTA ligands *cis* to the bromide, $^1J_{Pt-P} = 1971$ Hz), −48.69 (tt, due to the phosphorus atom of the PTA *trans* to the bromide, $^1J_{Pt-P} = 3309$ Hz). Electronic spectrum (H_2O): $\lambda_{max} = 290$ nm, $\varepsilon = 7307\ M^{-1}\ cm^{-1}$.

2.1.3. [Pt(N$_3$)(PTA)$_3$]N$_3$. A similar procedure for the synthesis of the [PtBr(PTA)$_3$]Br complex was followed. Addition of NaN_3 (213 mg, 3.3 mmol) to an aqueous solution (2 cm^3) of [PtCl(PTA)$_3$]Cl (80 mg, 0.1 mmol) gave a product which was recrystallized from methanol to yield a white product (30 mg, 37%). ^1H NMR (300 MHz, D_2O): δ 4.40 (d, 6H), 4.18 (s, 6H). $^{31}P\{^1H\}$ NMR (121.497 MHz, D_2O): δ −53.01 (t, broad peak). IR: $\nu(N_3)$ 2040 cm^{-1}. Electronic spectrum (H_2O): $\lambda_{max} = 285$ nm, $\varepsilon = 8800\ M^{-1}\ cm^{-1}$.

2.2. *X-ray crystallography*

X-ray diffraction data were collected at 173 K on a NONIUS Kappa CCD diffractometer using Mo-Kα radiation ($\lambda = 0.71073$ Å). Some 520 frames were collected and the total exposure time was 236 min with 27 sec exposure time per frame; 203 frames were recorded, each of width 0.9° in φ, followed by 317 frames of 0.9° width in ω (with κ not equal to 0). The unit cell was indexed from the first 12 frames and positional data were refined along with diffractometer constants to give final cell parameters. Integration and scaling (DENZO, SCALEPACK) [13] resulted in unique data sets corrected for Lorentz-polarization effects and for the effects of crystal decay and absorption by a combination of averaging of equivalent reflections and an overall volume and scaling correction. Empirical absorption corrections were applied using SADABS [14]. The experimental density of the crystal was determined by flotation in a solution of diiodomethane and benzene. The structure was solved by the heavy atom method and refined using full matrix least squares methods using SHELXS-97 [15] and SHELXL-97 [16] with F^2 being minimized. All non-hydrogen atoms were refined with anisotropic displacement parameters, while hydrogen atoms were constrained to parent sites, using a riding model. Hydrogen atom positions on the water solvent molecules were determined from the experimental data and Fourier maps. Molecular graphics were drawn using DIAMOND [17].

2.3. *Equilibrium studies*

Equilibrium and pH studies were all conducted using freshly prepared aqueous solutions of [PtCl(PTA)$_3$]Cl and NaCl at 25°C. All solutions were prepared to contain at least ten-fold excess NaCl. For all equilibrium constant determinations the platinum

and Cl^- concentrations were kept constant at 0.075 and 1.0 mM, respectively, while the various other halide and pseudohalide concentrations were varied in the 0.025–5.0 mM range. Absorbance spectra were recorded between 200 and 500 nm using 1 cm quartz cuvettes. At a selected wavelength, absorbance values were plotted against the halide concentration in order to obtain equilibrium constants using the appropriate formulas. Equilibrium constants were calculated from the absorbance versus concentration curves using the Scientist least-squares program [18]. In pH variation experiments a 1.0 M stock solution of trifluoromethanesulphonic (triflic) acid was prepared and different volumes of this solution were added to adjust pH. The final platinum and Cl^- concentrations used in these experiments were 0.075 and 20 mM, respectively.

3. Results and discussion

3.1. *Synthesis*

The reaction of a mixture of *cis*- and *trans*-$[PtCl_2(SMe_2)_2]$ with three equivalents of PTA in water results in the formation of $[PtCl(PTA)_3]Cl$ as reported previously [12]. Treatment of this complex with halides or pseudohalides, X^-, results in substitution of Cl^- according to (1),

$$[PtCl(PTA)_3]^+ + X^- \overset{K_L}{\rightleftharpoons} [PtX(PTA)_3]^+ + Cl^- \quad (X^- = Br^-, N_3^-, NCS^-, I^-) \tag{1}$$

K_L denotes the equilibrium constant for the cation. In this regard it has been demonstrated previously that $[PtCl(PTA)_3]^+$ reacts with I^- to form $[PtI(PTA)_3]^+$ and then in a consecutive reaction to form the unusual five-coordinate complex $[PtI_2(PTA)_3]$, whose crystal structure has been reported [19].

3.2. *X-ray crystallography*

Yellow crystals isolated from an aqueous reaction mixture of $[PtCl(PTA)_3]Cl$ and NCS^- were identified as $\{[Pt(NCS)(PTA)_3]NCS\}_3 \cdot 5H_2O$. Redissolution of these crystals in water gave an identical spectrum to that obtained during the equilibrium study of $[PtCl(PTA)_3]Cl$ and NCS^-, confirming that this is also the product of the reaction investigated as postulated above. The compound crystallizes in the triclinic space group $P\bar{1}$ with three platinum cations, three thiocyanate counterions and five solvent water molecules in the asymmetric unit. Each platinum cation consists of three PTA ligands, coordinated through the phosphorus atom, and a thiocyanate ligand through the nitrogen atom. The three platinum complexes are chemically equivalent but crystallographically different due to small variations in packing modes. The structure shows the Pt moiety to be distorted square planar with two PTA ligands *trans* to each other and the other PTA ligand bound *trans* to the nitrogen atom of the coordinated thiocyanate ligand (figure 1). The basic crystallographic and data collection parameters for $\{[Pt(NCS)(PTA)_3]NCS\}_3 \cdot 5H_2O$ are reported in table 1 while a complete set of atomic coordinates, bond lengths and angles is available

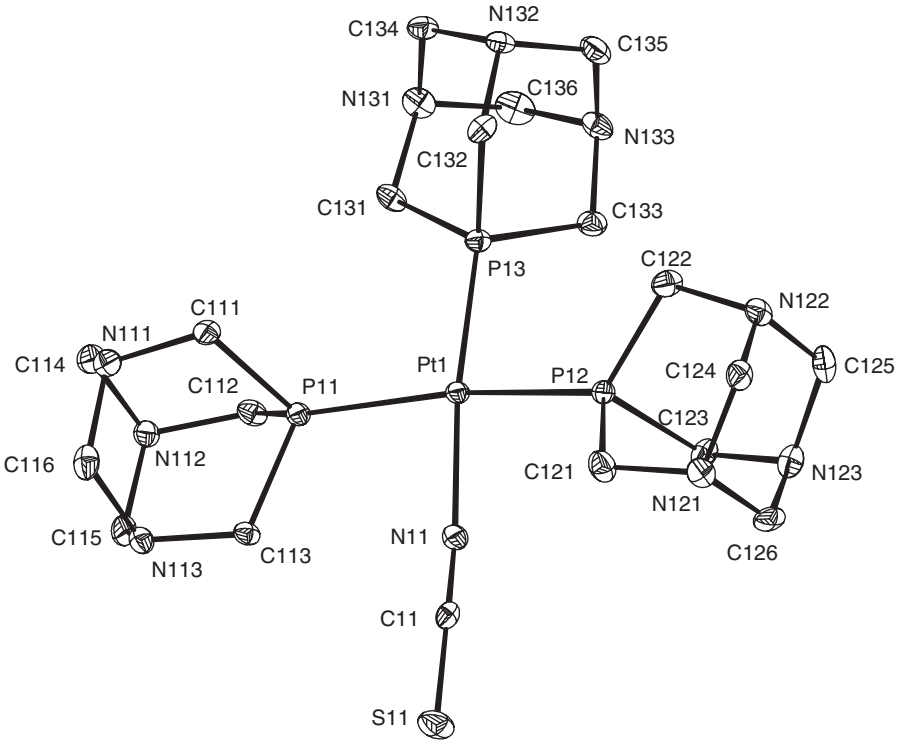

Figure 1. Molecular drawing of cation 1 of $\{[Pt(NCS)(PTA)_3]NCS\}_3 \cdot 5H_2O$ showing the numbering scheme with thermal ellipsoids drawn at the 30% probability level; cations 2 and 3 are similar. Hydrogen atoms, NCS^- anions and water molecules are omitted for clarity. In the numbering scheme the first digit refers to the number of the platinum(II) ion, the second to the number of the PTA ligand and the third to the number of the atom in the ligand.

from the Cambridge Crystallographic Data Centre. Further details regarding data request are given below.

Since $\{[Pt(NCS)(PTA)_3]NCS\}_3 \cdot 5H_2O$ crystallizes with three complex cations and free thiocyanate ligands in the asymmetric unit, there is complexity in the crystal packing. Figure 2 shows selective hydrogen bonding interactions in the system, indicated by dotted lines. The Pt–P bond distances of the phosphorus atoms of the PTA ligands *trans* to each other are significantly longer (average Pt–P distance = 2.3232(14) Å) than the Pt–P distances (average Pt–P distance = 2.2393(14) Å) of the phosphorus *trans* to the nitrogen atom (table 2 and figure 1). This is due to the large *trans* influence of the PTA ligands compared to that of nitrogen. The three independent cations in the asymmetric unit are almost identical with only small deviations in bond lengths and angles in the coordination sphere. Since the bond distances between the nitrogen atom of the free thiocyanate and the platinum (Pt(1)–N(1) = 5.493(7), Pt(2)–N(2) = 6.057(8), Pt(3)–N(3) = 5.758(6) Å, respectively), and the distance between the sulphur end of the free thiocyanate and platinum (S(1)–Pt(1) = 7.413(4), S(2)–Pt(2) = 4.647(3), S(3)–Pt(3) = 4.193(2) Å, respectively) are large, there is no interaction between them. However, there are interactions between the thiocyanate counterion and water molecules (N(1)–H(4A) = 2.062(7) Å) and between the nitrogen atom

Table 1. Crystallographic data for $\{[Pt(NCS)(PTA)_3]NCS\}_3 \cdot 5H_2O$.

Empirical formula	$C_{60}H_{118}N_{33}O_5S_6P_9Pt_3$
Formula weight	2438.2
Temperature (K)	173
Crystal system	Triclinic
Space group	$P\bar{1}$
a (Å)	14.9135(2)
b (Å)	15.2532(2)
c (Å)	22.7413(3)
α (°)	73.2012(6)
β (°)	78.5067(6)
γ (°)	61.7241(6)
Volume (Å^3)	4349.52(10)
Z	2
D_c (Mg m^{-3})	1.862
μ (mm^{-1})	5.189
F (000)	2428
θ range for data collection (°)	1.88–25.00
Index ranges	$0 \le h \le 17$, $-15 \le k \le 17$, $-26 \le l \le 27$
Reflections collected/unique	39540/14299 [$R_{int} = 0.05$]
Completeness to θ (°, %)	25.00, 93.3
Data/restraints/parameters	14299/0/1080
Goodness-of-fit on F^2	1.037
Final R indices [$I > 2\sigma(I)$]	$R_1 = 0.0328$, $wR_2 = 0.0639$
R indices (all data)	$R_1 = 0.0523$, $wR_2 = 0.0705$
$\Delta\rho_{max}$ and $\Delta\rho_{min}$ (e Å^{-3})	1.316 and −0.911

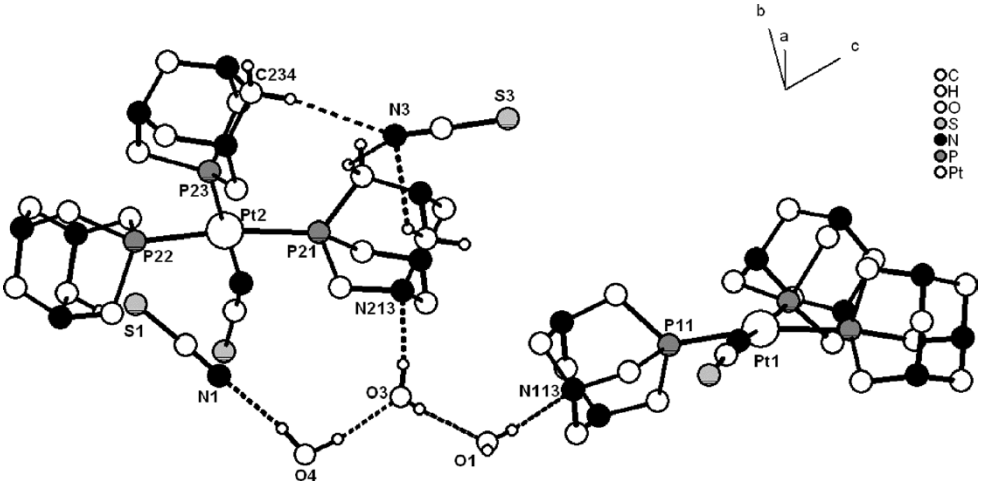

Figure 2. Diagram showing cations 1 and 2 of $\{[Pt(NCS)(PTA)_3]NCS\}_3 \cdot 5H_2O$ and selected hydrogen bonds in the solid state. Hydrogen atoms, except in atoms involved in hydrogen bonding, are omitted for clarity. Hydrogen bonding is indicated by dotted lines.

of PTA ligands and the solvent molecules (N(232)–H(2A) = 2.218(6), N(213)–H(3B) = 2.097(9) Å, respectively). These strong hydrogen bonds are shown in figure 2 together with weaker interactions between a carbon atom of the PTA ligand and the nitrogen atom of the free thiocyanate ligand. For all three cations, P–Pt–P angles (table 3) deviate significantly from 180° (166.94(5), 168.43(5) and 167.62(5)°), suggesting

Table 2. Selected bond lengths (Å) for $\{[Pt(NCS)(PTA)_3]NCS\}_3 \cdot 5H_2O$.

	Molecule 1 ($n=1$)	Molecule 2 ($n=2$)	Molecule 3 ($n=3$)
Pt(n)–P(n1)	2.3204(14)	2.3084(14)	2.3287(15)
Pt(n)–P(n2)	2.2966(13)	2.3353(13)	2.3496(15)
Pt(n)–P(n3)	2.2405(14)	2.2365(14)	2.2409(14)
Pt(n)–N(n1)	2.034(5)	2.051(4)	2.045(5)
N(n1)–C(n1)	1.155(6)	1.159(6)	1.151(6)
S(n1)–C(n1)	1.617(6)	1.617(5)	1.616(6)

Table 3. Selected bond angles (°) for $\{[Pt(NCS)(PTA)_3]NCS\}_3 \cdot 5H_2O$.

	Molecule 1 ($n=1$)	Molecule 2 ($n=2$)	Molecule 3 ($n=3$)
N(n1)–Pt(n)–P(n1)	86.70(12)	87.53(12)	86.58(13)
N(n1)–Pt(n)–P(n2)	83.81(12)	80.91(12)	81.33(13)
N(n1)–Pt(n)–P(n3)	170.94(13)	179.07(13)	178.88(14)
P(n1)–Pt(n)–P(n2)	166.94(5)	168.43(5)	167.62(5)
P(n1)–Pt(n)–P(n3)	96.83(5)	91.61(5)	92.48(5)
P(n3)–Pt(n)–P(n2)	93.89(5)	99.96(5)	99.63(5)
C(n1)–N(n1)–Pt(n)	171.1(5)	160.4(4)	169.5(5)
N(n1)–C(n1)–S(n1)	179.5(5)	178.4(5)	179.1(5)

Table 4. Comparison of structural parameters in $[PtX(PTA)_3]^+$ ($X = NCS^-$, Cl^-, I^-) complexes.

		$[Pt(NCS)(PTA)_3]^+$	$[PtCl(PTA)_3]^+$	$[Pt(I)_2(PTA)_3]$
Bond distances (Å)	Pt–P[a]	2.3232(14)	2.323(2)	2.317(2)
	Pt–P[b]	2.2393(14)	2.233(2)	2.251(1)
	Pt–X	2.043(5)	2.371(2)	2.719(1)
Bond angles (°)	(P–Pt–P)[a]	167.66(5)	167.0(1)	166.1(1)
	(P–Pt–P)[b]	93.64(5)	96(2)	96(2)
	(P–Pt–X)[a]	84.48(12)	83.3(1)	85.5(1)
	(P–Pt–X)[b]	176.30(13)	175.0(1)	156.3(1)
References		This work[c]	[20][d]	[19]

[a]Pt–P *trans* to each other. [b]Pt–P *trans* to X. [c]Crystallized as $\{[Pt(NCS)(PTA)_3]NCS\}_3 \cdot 5H_2O$. [d]Crystallized as the Cl^- salt.

significant steric interactions between PTA ligands. N(21)–Pt(2)–P(23) and N(31)–Pt(3)–P(33) bond angles are 179.07(13) and 178.88(14)°, respectively, and differ significantly from the N(11)–Pt(1)–P(13) bond angle, 170.94(13)°. This indicates that molecules 2 and 3 are more similar and slightly different to molecule 1.

The geometrical parameters of $\{[Pt(NCS)(PTA)_3]NCS\}_3 \cdot 5H_2O$ are compared with those of closely related structures found in the literature in table 4. It is noted that for some parameters of $\{[Pt(NCS)(PTA)_3]NCS\}_3 \cdot 5H_2O$, as compared with the other isostructural halide complexes, there is a slight difference in Pt–P bond distances *trans* to each other. However, in all structures there is an observable difference between Pt–P bonds *trans* to each other and Pt–P bonds *trans* to the halide. A general decrease of approximately 0.1 Å is noted and this is due to differences in *trans* influence. In the complexes listed, it is observed that there is an increase in the Pt–X bond distance with Pt–I being longest, due to the fact that the halide is large and thus causes further steric crowding.

The effective (θ_E) and Tolman (θ_T) cone angles of the PTA ligands were determined according to the Tolman model [9, 21]. Average values $\theta_E = 115.8^\circ$ and $\theta_T = 116.2^\circ$ deviate quite significantly from the previously reported value of 102° [22]. During the study, values for individual half-angles were determined using the graphics program DIAMOND [17]. In each case the largest half-angle to an atom (hydrogen in all cases) on individual substituents was used in the calculations. As the angles were measured from a point (2.28 Å from P, as per definition) to the position of the hydrogen atom, thus not involving the van der Waals radius, a correction [21] was applied.

3.3. *Stability and acid dissociation constants*

A stability check (electronic spectrum) conducted on an aqueous solution of $[PtCl(PTA)_3]^+$ indicated a slow spectroscopic change, believed to be related to hydrolysis since evaporation of solvent yielded the complex unchanged. Addition of free Cl^- consequently stabilized the solutions to such an extent that solution studies could be conducted over several hours, ensuring that Cl^- exchange is the only reaction investigated. There is an observed proton catalysis of PTA substitution (2) to form *cis*-$[PtCl_2(PTA)_2]$ when different concentrations of triflic acid are added to $[PtCl(PTA)_3]^+$ (figure 3a).

$$\underset{\text{I}}{[PtCl(PTA)_3]Cl} \overset{+H^+}{\rightleftharpoons} \underset{\text{II}}{[PtCl(PTA)_2(PTAH)]^{2+}} \underset{+PTAH}{\overset{+Cl^-}{\rightleftharpoons}} \underset{\text{III}}{cis\text{-}[PtCl_2(PTA)_2]} \qquad (2)$$

In more acidic solutions *cis*-$[PtCl_2(PTA)_2]$ is further protonated in a stepwise fashion resulting in the diprotonated PTA complex shown in (3), as verified by a single-crystal structure study [6].

$$\underset{\text{III}}{cis\text{-}[PtCl_2(PTA)_2]} \underset{K_{a2}}{\overset{+H^+}{\rightleftharpoons}} \underset{\text{IV}}{[PtCl_2(PTA)(PTAH)]^+} \underset{K_{a1}}{\overset{+H^+}{\rightleftharpoons}} \underset{\text{V}}{cis\text{-}[PtCl_2(PTAH)_2]^{2+}} \qquad (3)$$

Absorbance values (figure 3a) at different wavelengths were plotted against pH (see figure 3b), and were fitted to (4) [23] to obtain corresponding pK_a values;

$$A_{obs} = \frac{A_1[H^+]^2 + A_2K_{a1}[H^+] + A_3K_{a1}K_{a2}}{[H^+]^2 + K_{a1}[H^+] + K_{a1}K_{a2}} \qquad (4)$$

A_{obs} = total absorbance, A_1 = absorbance of *cis*-$[PtCl_2(PTAH)_2]^{2+}$, A_2 = absorbance of the *cis*-$[PtCl_2(PTA)_2]$, A_3 = absorbance of $[PtCl(PTA)_3]Cl$, K_{a1} and K_{a2} are acid dissociation constants of *cis*-$[PtCl_2(PTA)_2]$, (3). The experiments revealed that there are two regions where protonation is observed. Two pK_a values (table 5) at different wavelengths were determined using (4) yielding $pK_{a1} = 2.12$ (average pK_a) and $pK_{a2} = 3.5$ (average pK_a). Addition of acid resulted in one of the PTA ligands being protonated (3), corresponding to pK_{a1} and in the presence of Cl^- rapidly converts the resulting $[PtCl(PTAH)(PTA)_2]^{2+}$ to *cis*-$[PtCl_2(PTA)_2]$. The second protonation step pK_{a2} corresponds to protonation of one of the remaining PTA ligands in *cis*-$[PtCl_2(PTA)_2]$. Extensive studies have been reported on the effect of pH in water-soluble PTA complexes of ruthenium(II) and rhodium(I) [24–26]. Due to

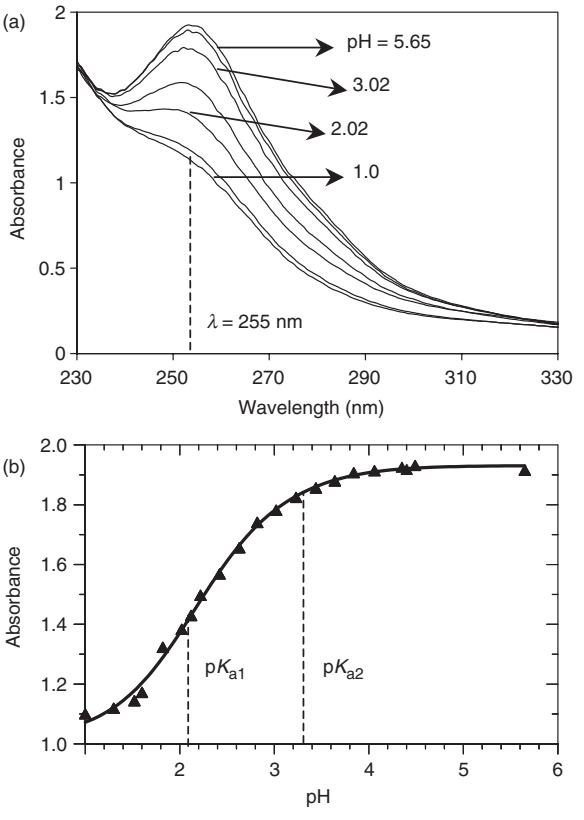

Figure 3. (a) Selected electronic spectra in aqueous solution (pH adjusted with triflic acid) showing the protonation behaviour of $[PtCl(PTA)_3]Cl$; $[Pt]_f = 0.075$ and $[Cl^-] = 20\,mM$, $T = 25^\circ C$ and pH = 1–6. (b) Absorbance *vs.* pH graph for $[PtCl(PTA)_3]Cl$; solid line represents the least-squares fit of data points at $\lambda = 255\,nm$ to (4).

Table 5. Values of pK_a obtained for the reaction of $[PtCl(PTA)_3]Cl$ with triflic acid at wavelengths of 255 and 276 nm. $[Pt] = 0.075\,mM$, $[Cl^-]$ (as NaCl) = 20 mM, pH = 1–6 and at $T = 25^\circ C$.

	$\lambda = 255\,nm$	$\lambda = 276\,nm$
pK_{a1}	2.1(1)	2.13(7)
pK_{a2}	3.3(8)	3.7(6)

the pH dependency of the complex the equilibrium substitution of the Cl^- ligand was investigated well above the second pK_a value to ensure that no substitution of the PTA ligands occurs.

3.4. *Equilibrium constant determinations*

Equilibrium constants obtained by reacting $[PtCl(PTA)_3]Cl$ with various halides and pseudohalides ($X^- = Br^-$, N_3^-, NCS^-) were well defined. Figure 4(a) illustrates overlay

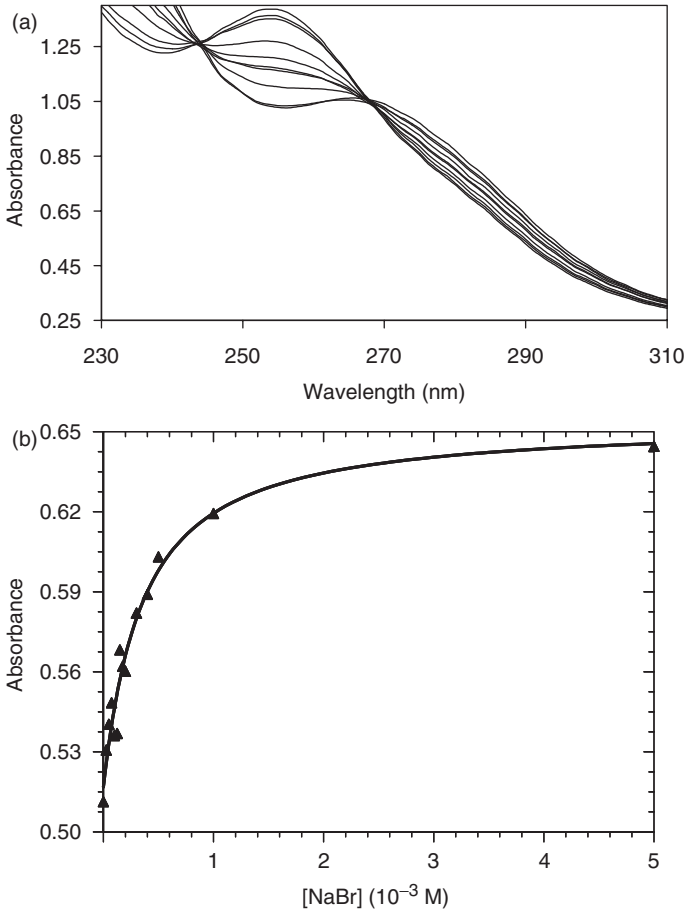

Figure 4. Graphs illustrating the aqueous behaviour of $[PtCl(PTA)_3]^+$ when reacted with different halides and pseudohalides. Electronic spectra overlay (a) $[Br^-] = 0$–5 mM, $[Pt]_f = 0.075$ mM and excess $[Cl^-] = 1$ mM, $T = 25°C$ and pH = 5.6. (b) Solid line represents least-squares fit of data points at $\lambda = 290$ nm to (5).

plots of absorbance versus wavelength when $[PtCl(PTA)_3]Cl$ is reacted with various ligands. The equilibrium reaction for the process is given in (1).

For determination of the equilibrium constants (5) [27] was used to fit the absorbance versus [X] data (see figure 4b),

$$A_{obs} = \frac{A_R[Cl^-] + (A_P)K[X]}{[Cl^-] + K[X]} \tag{5}$$

where A_{obs} = total absorbance, A_R = absorbance of the pure reactant, A_P = absorbance of the product, K = equilibrium constant, $[Cl^-]$ = concentration of added Cl^-, [X] = concentration of added halide or pseudohalide. When $[PtCl(PTA)_3]^+$ was reacted with several halides and pseudohalides ($X = Br^-$, N_3^-, NCS^-) well-defined equilibria were observed, thus forming the final products (1). An additional experiment involving the determination of equilibrium constants at constant ionic strength was done and

Table 6. Equilibrium constants for formation of $[PtX(PTA)_3]^+$ ($X = Br^-$, N_3^-, NCS^-, I^-) complexes at 25°C and pH = 5.6.

X	K[a]
Br^-	3.3(7)
N_3^-	11(2)
NCS^-	20(2)
I^-	11(3)[b]

[a]According to (1). [b]Ref. [19].

it gave similar results. Addition of halide or pseudohalide to $[PtCl(PTA)_3]^+$ results in rapid substitution of chloride to form $[PtX(PTA)_3]^+$. When $[PtCl(PTA)_3]Cl$ is dissolved in water, it was observed that it is unstable and hydrolyses, and excess chloride (as NaCl) was added to the aqueous solutions in all the equilibrium constant experiments to prevent hydrolysis and consequent decomposition. It is noted from table 6 that equilibrium constants for N_3^- and NCS^- are comparable, since in the structure isolated the NCS^- ligand is *N*-coordinated; this could be due to steric or electronic effects [28]. The increase from Br^- to I^- is in agreement with ligand strength of I^- versus Br^-.

Supplementary material

Crystallographic data have been deposited with the Cambridge Crystallographic Data Centre, CCDC No. 273283. Copies may be obtained free of charge from: The Director, CCDC, 12 Union Road, Cambridge CB2 1EZ, UK (Fax: +44 1223 336 033; E-mail: deposit@ccdc.cam.ac.uk) or via the internet at www.ccdc.cam.ac.uk/deposit.

Acknowledgements

Financial support from the research fund of the University of the Free State is gratefully acknowledged. The University of Cape Town is thanked for X-ray data collection. This work was also funded by the South African National Research Foundation under the Grant number GUN 2068915. The opinions, findings and conclusions or recommendations in this work are those of the authors and do not necessarily reflect the views of the NRF.

References

[1] L. Nádasdi, F. Joó. *Inorg. Chim. Acta*, **293**, 218 (1999).
[2] J. Kovács, T.D. Todd, J.H. Reibenspies, F. Joó, D.J. Darensbourg. *Organometallics*, **19**, 3963 (2000).
[3] B.M. Novak, R.H. Grubbs. *J. Am. Chem. Soc.*, **110**, 7542 (1988).
[4] K.V. Katti. *Current Science*, **70**, 219 (1996).
[5] D.J. Daigle, A.B. Pepperman Jr, S.L. Vail. *J. Heterocyclic Chem.*, **17**, 407 (1974).
[6] D.J. Darensbourg, T.J. Decuir, N.W. Stafford, J.B. Robertson, J.D. Draper, J.H. Reibenspies. *Inorg. Chem.*, **36**, 4218 (1997).

[7] (a) D.J. Darensbourg, F. Joó, M. Kannisto, A. Kathó, J.H. Reibenspies, D.J. Daigle. *Inorg. Chem.*, **33**, 200 (1994); (b) D.J. Darensbourg, F. Joó, M. Kannisto, A. Kathó, J.H. Reibenspies. *Organometallics*, **11**, 1990 (1992); (c) F. Joó, L. Nádasdi, A.C. Bényei, D.J. Darensbourg. *J. Organomet. Chem.*, **512**, 45 (1996).
[8] E.C. Alyea, K.J. Fisher, S. Johnson. *Can. J. Chem.*, **67**, 1319 (1989).
[9] C.A. Tolman. *Chem. Rev.*, **77**, 313 (1977).
[10] D.J. Daigle, A.B. Pepperman Jr, S.L. Vail. *J. Heterocyclic Chem.*, **11**, 407 (1974).
[11] D.J. Daigle, T.J. Decuir, J.B. Robertson, D.J. Darensbourg. *Inorg. Synth.*, **32**, 40 (1998).
[12] S. Otto, A. Roodt, W. Purcell. *Inorg. Chem. Commun.*, **1**, 415 (1998).
[13] Z. Otwinowski, W. Minor. *DENZO and SCALEPACK*, *International Tables for Crystallography*, Vol. F, Kluwer, Dordrecht (2000).
[14] G.M. Sheldrick. *SADABS, Program for Empirical Absorption Correction for Area Detector Data*, University of Göttingen, Germany (1996).
[15] G.M. Sheldrick. *SHELXS-97, Program for Crystal Structure Determination*, University of Göttingen, Germany (1997).
[16] G.M. Sheldrick. *SHELXL-97, Program for Crystal Structure Refinement*, University of Göttingen, Germany (1997).
[17] K. Brandenburg, M. Berndt. *DIAMOND. Release 2.1e., Program for Molecular Graphics*, Crystal Impact, Bonn, Germany (2001).
[18] *Scientist for Windows, Least-squares Parameter Estimation, Version 4.00.950*, MicroMath (1990).
[19] S. Otto, A. Roodt. *Inorg. Chem. Commun.*, **4**, 49 (2001).
[20] M.M. Muir, J.A. Muir, E.C. Alyea, K.J. Fisher. *J. Cryst. Spectr. Res.*, **23**, 745 (1993).
[21] S. Otto, A. Roodt, J. Smith. *Inorg. Chim. Acta*, **303**, 295 (2000).
[22] J.R. DeLerno, L.M. Trefonas, M.Y. Darensbourg, R.J. Majeste. *Inorg. Chem.*, **15**, 816 (1976).
[23] A. Roodt, J.G. Leipoldt, L. Helm, A.E. Merbach. *Inorg. Chem.*, **31**, 2864 (1992).
[24] F. Joó, J. Kovács, A.C. Bényei, A. Kathó. *Angew. Chem. Int. Ed.*, **37**, 969 (1998).
[25] F. Joó, J. Kovács, A.C. Bényei, A. Kathó. *Catalysis Today*, **42**, 441 (1998).
[26] F. Joó, J. Kovács, A.C. Bényei, L. Nádasdi, G. Laurenczy. *Chem. Eur. J.*, **7**, 193 (2001).
[27] M. Plutino, S. Otto, A. Roodt, L.I. Elding. *Inorg. Chem.*, **38**, 1233 (1999).
[28] J.L. Burmeister, F. Basolo. *Inorg. Chem.*, **3**, 1587 (1964).